

Received May 11, 2021, accepted May 30, 2021, date of publication June 10, 2021, date of current version June 23, 2021.

Digital Object Identifier 10.1109/ACCESS.2021.3088274

# Analysis of Measurement Accuracy of Multi-Objective Normalization Algorithm Under Different Reference Systems

SI-LIANG LI<sup>ID</sup>, HAI-JIANG LIU, ZE-YU XU, AND JIN-SONG LIU

School of Mechanical Engineering, Tongji University, Shanghai 201804, China

Corresponding author: Hai-Jiang Liu (haijiangliu317@gmail.com)

This work was supported in part by the Joint Fund Project for Innovation and Development of China's Automobile Industry under Grant U1764259.

**ABSTRACT** Aiming at the problem that the base coordinate system of industrial robot is not unified with the center coordinate system of tool, and it is impossible to input the action position in the robot teaching device, this paper adopts ROMER HEXAGON METROLOGY 7530SE three-coordinate measuring instrument as the robot measuring equipment and proposes a multi-objective normalization algorithm. In this paper, the reliability of the multi-objective normalization algorithm is verified by the experiment, and the measurement accuracy difference of the multi-objective normalization algorithm under different reference systems is studied. The results have shown that the accuracy of the system reaches 0.8 mm and the root mean square (RMS) value is maintained at 0.3-0.7 mm when the engine is taken as the reference coordinate system within the robot's 0-50mm motion stroke. When the body-in-white is used as the reference coordinate system, the accuracy of the system can reach 2.2 mm, the RMS value can be maintained at 1.0-1.8mm. The reasons for good accuracy and stability of the measurement system established with the engine as the reference coordinate are analyzed. The multi-objective normalization algorithm proposed in this paper has high engineering universality, and the accuracy analysis of the algorithm under different reference system has guiding significance for the selection of reference coordinate system of measurement system.

**INDEX TERMS** Error analysis, robot motion, measurement technology, measurement accuracy, multi-objective normalization algorithm.

## I. INTRODUCTION

With the rise of intelligent manufacturing, industrial robots are increasingly used in the fields of industrial manufacturing and auxiliary motion error accuracy measurement. When the robot assists the components motion to measure the components motion accuracy, the base coordinate system of the robot is not unified with the tool center point (TCP) coordinate system, it is impossible to input the components target position in the robot teaching device, which limits the application of the robot in the field of industrial measurement. Since this problem, many scholars have carried out relevant research. For example, a method to unify the sensor coordinate system and the target coordinate system by using mechanical constraints is proposed. The method realizes the coordinate conversion of two coordinate systems, and when the transformation coordinate system is applied to actual

measurement, the accuracy is analyzed [1]. An automatic calibration method using real-time 3D simulation sensors is proposed. The method obtains the rigid body coordinate transformation matrix through real-time correlation between virtual sensors and real sensors [2]. In order to obtain the target posture of the robot, Monte Carlo theory and posture transformation matrix are combined to solve the terminal posture transformation matrix [3]. Aiming at the problem that the end of industrial robot cannot be measured directly, the conversion between different coordinate systems is realized by laser target, and the deviation between the end position displayed by robot teaching device and the actual end position is measured [4]. Aiming at the problem of poor conditions matrix that may occur when solving coordinate transformation with point cloud equation, a coordinate transformation solution scheme based on geometric transformation is proposed. Experimental verification shows that the proposed method improves the position accuracy of the robot manipulator by 45.8% [5]. In order to improve the calibration

The associate editor coordinating the review of this manuscript and approving it for publication was Luigi Biagiotti<sup>ID</sup>.

accuracy of industrial robots, the error parameter model are found by Jacobian linear iteration, and the robot motion accuracy is calibrated with less than 50 configurations. The calibration efficiency is verified by laser tracker and optical coordinate measuring machine [6].

In this paper, a multi-objective normalization algorithm is proposed. Which maps the robot tool center point coordinate system to the robot base coordinate system through the coordinate transformation matrix, and realizes the purpose of the robot teaching device directly inputting the target position of the load components. Furthermore, the reliability of the multi-objective normalization algorithm is verified through the experiment and the measurement accuracy of the algorithm under different reference system is studied and analyzed.

## II. MULTI-OBJECTIVE NORMALIZATION ALGORITHM

In this paper, the measurement system includes KUKA KR210 R2700 robot (hereinafter referred to as robot), engine, ROMER HEXAGON METROLOGY 7530SE three-coordinate measuring instrument (hereinafter referred to as Faro) and other components, which introduces the coordinate systems such as robot base coordinate system OR, robot tool coordinate system OT, Faro measuring coordinate system OF, body-in-white coordinate system OB, and engine coordinate system OE. Because many objects and measurement coordinate are introduced, in order to facilitate the robot teaching device control the motion of the robot tool coordinate system, a Multi-objective Normalization Algorithm is proposed in this paper.

Unification of Feature Points in Multiple Coordinate Systems [7]–[15] is the core of the Multi-objective Normalization Algorithm. The mathematical tool used in the algorithm is coordinate transformation matrix [16]–[19]. The transformation matrix structure includes rotation matrix and displacement matrix. The specific form of transformation matrix is shown in Fig. 1.

According to the structure of the transformation matrix, assuming that there are four points  $P_i (i = 1, 2, 3, 4)$  in the coordinates system A and B, and the coordinates are  $P_i^A$  and  $P_i^B$  respectively, the transformation matrix  $T_{A-B}$  can be solved according to the Eq.(1).

$$P_i^A \cdot T_{A-B} = P_i^B \quad (i = 1, 2, 3, 4) \quad (1)$$

In this paper, robot base coordinate system OR, robot tool coordinate system OT, Faro measuring coordinate system OF, body-in-white coordinate system OB, and engine coordinate system OE are introduced into the measurement system. The relationship between the 5 coordinate system in the system is shown in Fig.2.

According to Fig. 2, the flow chart of the multi-objective normalization algorithm coordinate system transformation is shown in Fig. 3, and the specific operation flow is as follows:

Step1: Acquiring the OT to OR transformation matrix  $T_{T-R}$

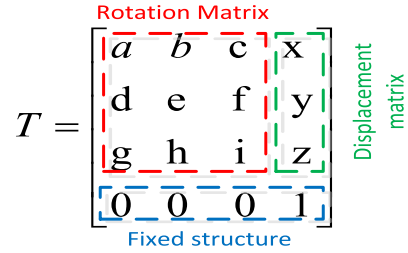


FIGURE 1. Transformation matrix structure.

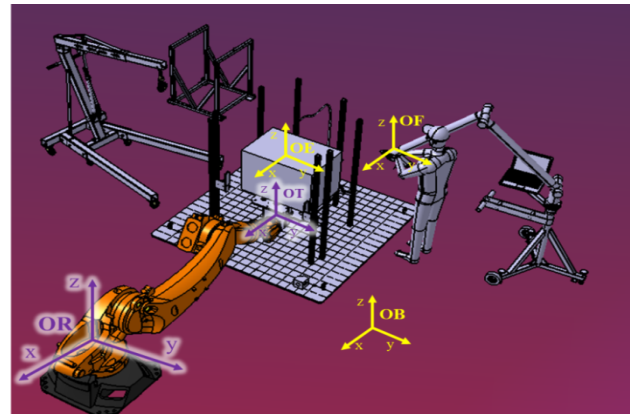
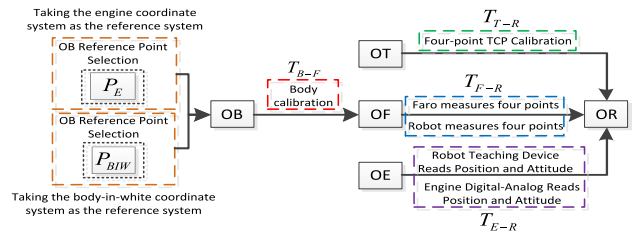


FIGURE 2. Schematic diagram of coordinate systems in measurement system.



Note:  $P_E$  is the measured calibration value of the engine;  $P_{BIW}$  is the measured calibration value of the body-in-white.

FIGURE 3. Flow chart of coordinate system transformation relation of multi-objective normalization algorithm.

In order to realize the purpose of converting the coordinates in OT into OR and obtain the conversion matrix  $T_{T-R}$ , the four-point method is used [20], [25]. The feature point A is obtained by operating the robot to measure the measuring block. Among them, the measuring block is shown in Fig.4.

Step2: Acquiring the OB to OR transformation matrix  $T_{B-R}$

In order to obtain the transformation matrix  $T_{B-R}$ , in this paper, the solution is divided into two steps. ① Faro is used to measure the coordinates of four feature points on the engine, and the actual measured values of feature points in OB are compared and calculated to obtain the conversion matrix  $T_{B-F}$ . ② The feature points coordinates of the measuring block in OR system is obtained by robot, and the feature points coordinates of the measuring block in OF system is measured by Faro, the transformation matrix  $T_{F-R}$  is obtained by performing mathematical operations on two sets of coordinates. Finally, the transformation matrix

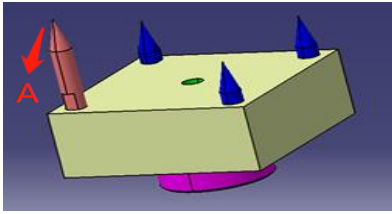


FIGURE 4. Schematic diagram of measuring block structure.

$T_{B-R}$  is obtained, according to the obtained transformation matrix  $T_{B-F}$  and  $T_{F-R}$ , combining the mathematical operation  $T_{B-R} = T_{B-F} \cdot T_{F-R}$ .

Step3: Obtain the posture of the engine in the OT

In order to control the engine to complete pose transformation by changing the input coordinates of the robot teaching device, it is necessary to obtain the pose of the engine in OT. The TCP point pose in OR is obtained by the robot teaching device, and the coordinates of the engine four feature points are obtained by Faro, according to  $E_T = E_R \cdot T_{R-T}$ , the pose  $E_T$  is solved. Where  $E_R$  is the pose of engine in OB and  $E_R = E_B \cdot T_{B-R}$ . Among them,  $E_B$  is the theoretical calibration values of four feature points on the engine in OB under the initial state,  $T_{R-T}$  is the transformation matrix from OR to OT.

Step4: Compute output motion data

The input of the multi-objective normalization algorithm is the motion transformation matrix  $M_B$  of the engine in OB and the theoretical calibration values  $E_B$  of four feature points on engine in OB at the initial state. The output of the algorithm proposed in this paper is target pose  $TCP - O_R$  of TCP points in OR system after robot action.

According to the matrix transformation relation obtained in step1, 2and 3, it can be deduced that:

$$E - O_B = M_B \cdot E_B \quad (2)$$

$$E - O_R = E - O_B \cdot T_{B-R} \quad (3)$$

$$TCP - O_R = E - O_R \cdot T_{R-T} \quad (4)$$

In Eq.(2),  $E - O_B$  is the engine target pose in OB and  $E - O_R$  is the engine target pose in OR. According to formula (4),  $TCP - O_R$  is obtained, and the purpose robot teaching device directly inputting the target position of the load components is realized.

### III. ACCURACY ANALYSIS OF FEATURE POINTS MEASUREMENT UNDER DIFFERENT REFERENCE SYSTEMS

In the experiment of simulating automobile shaking with robot load engine, in order to obtain the position accuracy of engine shaking, the position of engine characteristic points is measured. At present, the measurement method widely used in industry is to select the body-in white as the reference coordinate system. If the engine feature points do not meet the system position accuracy, the robot is controlled to move the engine to ensure that it is in the correct position in the automobile system. However, using body-in-white as a reference coordinate system to analyze the accuracy of engine shaking position will introduce the manufacturing error

of body-in-white, which will increase the measurement error. Therefore, this paper introduces the engine as the reference coordinate system, the accuracy of the measurement system under the two reference coordinate systems are compared and analyzed, and the reasons for the error reduction of the measurement system are explained.

#### A. ESTABLISHING MEASUREMENT SYSTEM WITH ENGINE AS REFERENCE SYSTEM

When the measurement system is established with the engine as the reference system, using Poly Works software and Faro to measure the coordinate of the feature points on the engine (the position of the feature points on the engine is shown in Fig. 5). The actual measurement coordinates of four points on engine are aligned with their theoretical coordinates in OB in Poly Works software. When the alignment error is less than 0.3 mm (ensuring that the sum of accumulated errors of the whole measurement system is kept within 1mm), the alignment operation is regarded as completed.

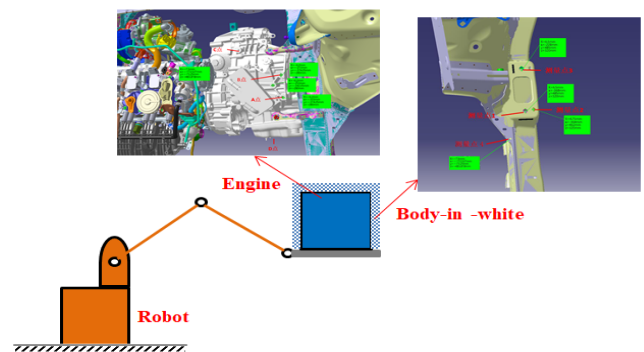


FIGURE 5. Location diagram of feature points on engine and body-in-white.

After the measurement system is established with the engine coordinate system as the reference system, the target pose  $TCP - O_R$  of the robot TCP point in OR is solved according to the Multi-objective normalization algorithm. According to the motion logic of  $TCP - O_R$ , on the basis of the initial theoretical position of engine digital model, coordinate transformation was carried out to solve the theoretical coordinates of feature points after motion. The theoretical coordinates of motion feature points are compared with the feature points position coordinates measured by Faro to obtain the measurement accuracy error of the measurement system.

#### B. ESTABLISHING MEASUREMENT SYSTEM WITH BODY-IN-WHITE AS REFERENCE SYSTEM

When the measurement system is established with the body-in-white as the reference system, firstly, it is necessary to ensure the position of engine which is loaded by robot at the initial position (the theoretical initial position of engine and body-in-white), and then the coordinate of body-in-white feature points is measured by Faro. Finally, the feature points actual measured coordinates of body-in-white and their

theoretical coordinates of digital model is aligned in Poly Works software. When the alignment error of feature points was less than 0.5 mm (due to the limitation of the manufacturing accuracy of the body-in-white, the allowable maximum alignment error is determined to be 0.5 mm), the alignment is regarded as complete.

When establishing measurement system with body-in-white as the reference system, it is necessary to ensure the position of engine which is loaded by robot at the initial position. Then the Multi-objective normalization algorithm is used to control the motion of engine, on the basis of the initial theoretical coordinates of engine, coordinate transformation was carried out according to the motion logic of the robot. Engine feature points theoretical coordinates after motion are solved, measurement accuracy error of the measurement system is obtained by comparing the theoretical coordinates with the position coordinates of feature points measured by Faro.

**IV. EXPERIMENT AND ANALYSIS**

The measurement system in this paper mainly includes robot, engine, Faro, test bench and other components. The site diagram of the measurement system is shown in Fig. 6.

According to the measurement scheme described above, the measurement system is established by taking engine and body-in-white system as the reference system respectively. The actual measurement coordinates of engine four feature points and their theoretical coordinates are compared respectively in the measurement system. The maximum deviation of four feature points is selected as the measurement system accuracy error for this robot stroke.

In the measurement system constructed with the engine and body-in-white as the reference coordinate system, the measurement accuracy error result is shown in Fig. 7.

In Fig. 7, from a macroscopic point of view, when the measurement system takes body-in-white as the reference system, the accuracy error of the measurement system can reach 2.2 mm. When the measurement system takes engine as the reference system, the accuracy error of the measurement system reaches 0.8 mm. In addition, it can be seen that when the measurement system is established with the engine as the reference system, the accuracy error of the measurement system is smaller and the measurement system is more stable. From a microscopic point of view, when the measurement system is constructed with body-in-white as the reference system and the robot motion with a stroke of 10-20mm, the accuracy error of the measurement system begins to show discrete trend, and the discrete trend is most obvious when the robot moves with a stroke of 30-40mm. When the measurement system takes engine as the reference system, the accuracy error of the measurement system shows convergence trend, and there is no discretization phenomenon of the measurement accuracy error, in addition, the measurement accuracy error rises steadily with the robot motion stroke increase.

In order to quantitatively analyze the accuracy error stability of the measurement system, the root mean square

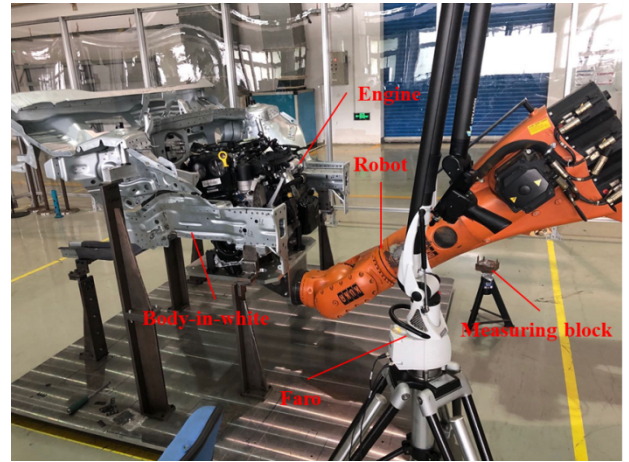


**FIGURE 6. Site diagram of measurement system.**

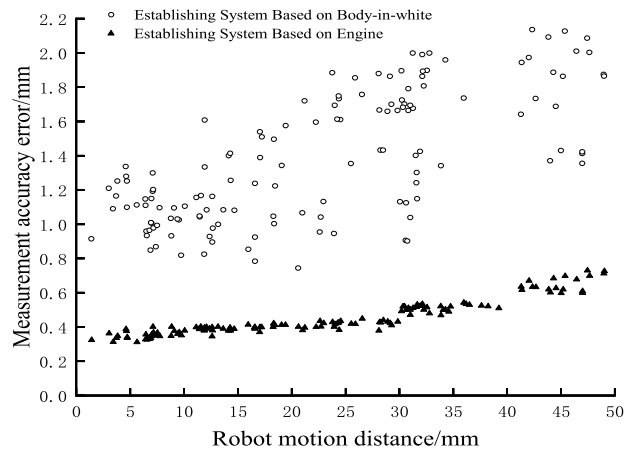


**FIGURE 7. Measurement accuracy error of multi-objective normalization algorithm under different reference systems.**

error (RMS) is introduced as the performance evaluation standard, and its calculation formula as follows:

$$E_{RMS} = \sqrt{\frac{1}{N} \sum_{i=1}^N \delta_{x_i}^2} \tag{5}$$

Among them,  $\delta_{x_i}$  is the measurement accuracy error of the measurement system in reference coordinate system, and  $N$  is the number of robot movements.

According to Fig. 7 and Eq. (5), the measurement system accuracy error analysis table is obtained as follows:

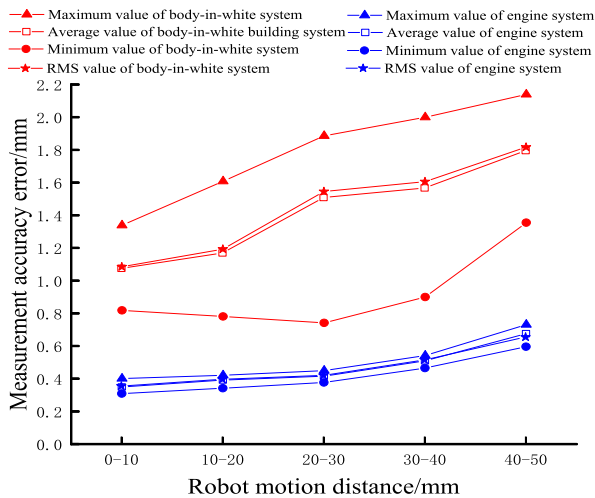
In table 1, from the macroscopic point of view, when the measurement system is established with body-in-white as the reference frame, the RMS value of the measurement system is larger in the whole robot motion stroke. Which shows that the measurement system error, when the measurement system is built on body-in-white, has a large jump and the stability is poor during the whole robot motion stroke. From the microscopic point of view, when the measurement is built on body-in-white, the RMS value of the measurement system in each motion stroke is bigger than the measurement system which is built on engine. It shows that in each motion stroke

**TABLE 1. Accuracy error analysis table of measurement system.**

Unit: mm	Take the engine as the reference system					Take the body-in-white as the reference system						
	0-10	10-20	20-30	30-40	40-50	0-50	0-10	10-20	20-30	30-40	40-50	0-50
Motion stroke												
Maximum	0.4012	0.4211	0.4494	0.5416	0.7310	0.7310	1.3368	1.6059	1.8838	1.9976	2.1371	2.1371
Minimum	0.3116	0.3446	0.3795	0.4681	0.5989	0.3116	0.8192	0.7818	0.7429	0.9006	1.3558	0.7429
Average	0.3509	0.3933	0.4169	0.5108	0.6771	0.4698	1.0755	1.1697	1.5091	1.5674	1.7962	1.4235
RMS	0.3516	0.3936	0.4173	0.5119	0.6517	0.4607	1.0839	1.1919	1.5446	1.6050	1.8156	1.4315

of the robot, when the measurement system is built on the engine, the consistency of system is great, and the stability is better.

In order to further analyze the trend of Multi-objective normalization algorithm measurement accuracy under different reference system, the trend diagram of measurement accuracy error is obtained as shown in Fig. 8.

**FIGURE 8. Trend change of measurement accuracy error of Multi-objective normalization algorithm under different reference systems.**

From the Fig. 8, it can be seen that from a macroscopic point of view, when the measurement system is established on body-in-white, the measurement accuracy error of the system is higher than the system is built on engine. Secondly, when the measurement system is established on body-in-white, the error distribution interval of the system is larger than the system is built on engine, which indicates that the stability of the measurement system is built on body-in-white is poor. From a microscopic point of view, in a certain motion stroke of robot, when the measurement system is established on the engine, the error distribution interval of the system is much smaller than the measure system is built on body-in-white, which indicates that in a single motion stroke, the measurement system is established on engine has higher measurement accuracy and stronger stability.

According to the experimental conditions and steps, combined with the principle of Multi-objective normalization algorithm, the reasons for high measurement accuracy and

great stability of the measurement system is built on engine are analyzed as follows:

(a) The manufacturing accuracy of body-in-white is poor. Although the finished round holes on body-in-white are selected as the feature points of body-in-white system, it still introduces large measurement errors and coordinate alignment errors.

(b) When the measurement system is built on engine, the initial condition of the Multi-objective normalization algorithm is to ensure that the initial position of engine is the theoretical relative position between the engine and the body-in-white. Due to high motion accuracy of the robot, this relative position is fully guaranteed, and the position is the initial position when the measurement system is built on engine. In addition, there is no body-in-white manufacturing errors are introduced in the process, so that the measurement system which is built on engine has high measurement accuracy and great measurement stability.

## V. CONCLUSION

In this paper, Multi-objective normalization algorithm was proposed to solve the problem the base coordinate system of robot and its tool center point coordinate system are not unified, in addition, the target action position of components which was loaded by robot cannot be directly input into robot teaching device. At the same time, the measurement accuracy error of Multi-objective normalization algorithm under different reference systems was studied.

The research result has shown that, within the 0-50mm motion stroke of robot, when the measurement system was built on body-in-white as the reference system, the measurement accuracy error reached 2.2 mm and the RMS value was maintained at 1.0-1.8 mm. When the measurement system was built on engine as the reference system, the measurement accuracy error reached 0.8 mm and the RMS value was maintained at 0.3-0.7 mm. The result has shown that when the measurement system was built on engine as the reference system, the accuracy error of the measurement system was small and the stability was great. When the measurement system was built on body-in-white, the measurement accuracy error was large and the stability was poor due to the poor manufacturing accuracy of body-in-white and the Multi-objective normalization algorithm introduces the manufacturing error twice when determining the initial position. The multi-objective normalization algorithm proposed in this

paper has high engineering universality, and the accuracy error analysis of the multi-objective normalization algorithm under different reference systems has guiding significance for the selection of reference coordinate system in engineering field.

## REFERENCES

- [1] Y. Wang et al., "Global calibration of visual inspection system based on universal robots," *Opt. Precis. Eng.*, no. 12, 2009.
- [2] Y. Ninomiya, Y. Arita, R. Tanaka, T. Nishida, and N. I. Giannoccaro, "Automatic calibration of industrial robot and 3D sensors using real-time simulator," in *Proc. Int. Conf. Inf. Commun. Technol. Robot. (ICT-ROBOT)*, Sep. 2018, pp. 1–4.
- [3] J. Li, F. Zhao, X. Li, and J. Li, "Analysis of robotic workspace based on Monte Carlo method and the posture matrix," in *Proc. IEEE Int. Conf. Control Robot. Eng. (ICCRE)*, Apr. 2016, pp. 1–5.
- [4] L. Li, C. Zhao, C. Li, and S. Qin, "End position detection of industrial robots based on laser tracker," *Instrum. Mesure Métrologie*, vol. 18, no. 5, pp. 459–464, Nov. 2019.
- [5] B. Liu, F. Zhang, X. Qu, and X. Shi, "A rapid coordinate transformation method applied in industrial robot calibration based on characteristic line coincidence," *Sensors*, vol. 16, no. 2, p. 239, Feb. 2016.
- [6] A. Nubiola, M. Slamani, A. Joubair, and I. A. Bonev, "Comparison of two calibration methods for a small industrial robot based on an optical CMM and a laser tracker," *Robotica*, vol. 32, no. 3, p. 447, 2014.
- [7] J. Yang, Q. Zhou, W. Cao, and Z. Yi, "Algorithm and realization of robotic end orientation equivalent similarity transformation based on rodrigues," in *Proc. 7th Int. Conf. Inf., Commun. Netw. (ICICN)*, Apr. 2019, pp. 175–179.
- [8] H. N. M. Shah, M. Sulaiman, A. Z. Shukor, and Z. Kamis, "An experiment of detection and localization in tooth saw shape for butt joint using KUKA welding robot," *Int. J. Adv. Manuf. Technol.*, vol. 97, nos. 5–8, pp. 3153–3162, Jul. 2018.
- [9] R. C. Luo and H. Wang, "Automated tool coordinate calibration system of an industrial robot," in *Proc. IEEE/RSJ Int. Conf. Intell. Robots Syst. (IROS)*, Oct. 2018, pp. 5592–5597.
- [10] H. Sung, S. Lee, and D. Kim, "A robot-camera hand/eye self-calibration system using a planar target," in *Proc. IEEE ISR*, Oct. 2013, pp. 1–4.
- [11] Y. J. Ren, J. G. Zhu, X. Y. Yang, and S. H. Ye, "Measurement robot calibration model and algorithm based on distance accuracy," *Acta Metrolog. Sinica*, vol. 29, no. 3, pp. 198–202, 2008.
- [12] Z. Bo, W. Zhenzhong, and Z. Guangjun, "Rapid coordinate transformation between a robot and a laser tracker," *Chin. J. Sci. Instrum.*, vol. 31, no. 9, pp. 1986–1990, 2010.
- [13] A. R. Norman, A. Schönberg, I. A. Gorfach, and R. Schmitt, "Validation of iGPS as an external measurement system for cooperative robot positioning," *Int. J. Adv. Manuf. Technol.*, vol. 64, nos. 1–4, pp. 427–446, Jan. 2013.
- [14] F. J. Brosed, J. Santolaria, J. J. Aguilar, and D. Guillomía, "Laser triangulation sensor and six axes anthropomorphic robot manipulator modelling for the measurement of complex geometry products," *Robot. Comput.-Integr. Manuf.*, vol. 28, no. 6, pp. 660–671, Dec. 2012.
- [15] J. Santolaria, D. Guillomía, C. Cajal, J. Albajez, and J. Aguilar, "Modelling and calibration technique of laser triangulation sensors for integration in robot arms and articulated arm coordinate measuring machines," *Sensors*, vol. 9, no. 9, pp. 7374–7396, Sep. 2009.
- [16] G. Du and P. Zhang, "Online robot calibration based on vision measurement," *Robot. Comput.-Integr. Manuf.*, vol. 29, no. 6, pp. 484–492, Dec. 2013.
- [17] L. C. Básaca-Preciado, O. Y. Sergiyenko, J. C. Rodríguez-Quinonez, X. García, V. V. Tyrsa, M. Rivas-Lopez, D. Hernandez-Balbuena, P. Mercorelli, M. Podrygalo, A. Gurko, I. Tabakova, and O. Starostenko, "Optical 3D laser measurement system for navigation of autonomous mobile robot," *Opt. Lasers Eng.*, vol. 54, pp. 159–169, Mar. 2014.
- [18] L. Wu, X. Yang, K. Chen, and H. Ren, "A minimal POE-based model for robotic kinematic calibration with only position measurements," *IEEE Trans. Autom. Sci. Eng.*, vol. 12, no. 2, pp. 758–763, Apr. 2015.
- [19] P. Huang, F. Zhang, J. Cai, D. Wang, Z. Meng, and J. Guo, "Dexterous tethered space robot: Design, measurement, control, and experiment," *IEEE Trans. Aerosp. Electron. Syst.*, vol. 53, no. 3, pp. 1452–1468, Jun. 2017.
- [20] J. G. Mangelson, D. Dominic, R. M. Eustice, and R. Vasudevan, "Pairwise consistent measurement set maximization for robust multi-robot map merging," in *Proc. IEEE Int. Conf. Robot. Autom. (ICRA)*, May 2018, pp. 2916–2923.
- [21] G. Xiong, Y. Ding, L. Zhu, and C.-Y. Su, "A product-of-exponential-based robot calibration method with optimal measurement configurations," *Int. J. Adv. Robot. Syst.*, vol. 14, no. 6, Nov. 2017, Art. no. 172988141774355.
- [22] N. Mu, K. Wang, Z. Xie, and P. Ren, "Calibration of a flexible measurement system based on industrial articulated robot and structured light sensor," *Opt. Eng.*, vol. 56, no. 5, May 2017, Art. no. 054103.
- [23] K. Merckaert, A. De Beir, N. Adriaens, I. El Makrini, R. Van Ham, and B. Vanderborgh, "Independent load carrying and measurement manipulator robot arm for improved payload to mass ratio," *Robot. Comput.-Integr. Manuf.*, vol. 53, pp. 135–140, Oct. 2018.
- [24] B. A. N. Campos and J. M. S. T. Motta, "Online measuring of robot positions using inertial measurement units, sensor fusion and artificial intelligence," *IEEE Access*, vol. 9, pp. 5678–5689, 2021.
- [25] M. Y. Moemen, H. Elghamrawy, S. N. Givigi, and A. Noureldin, "3-D reconstruction and measurement system based on multimobile robot machine vision," *IEEE Trans. Instrum. Meas.*, vol. 70, pp. 1–9, 2021.
- [26] R. Saegusa, H. Ito, and D. M. Duong, "Human-care rounds robot with contactless breathing measurement," in *Proc. Int. Conf. Robot. Autom. (ICRA)*, May 2019, pp. 6172–6177.
- [27] R. Danzl, T. Lankmair, A. Calvez, and F. Helmi, "Robot solutions for automated 3D surface measurement in production," in *Proc. 18th Int. Congr. Metrology*, 2017, p. 15002.
- [28] N. Mostashiri, C. Cheng, J. Wang, J. S. Dhupia, and W. Xu, "In-vitro measurement of reaction forces in the temporomandibular joints using a redundantly actuated parallel chewing robot," in *Proc. IEEE/ASME Int. Conf. Adv. Intell. Mechatronics (AIM)*, Jul. 2019, pp. 1467–1472.



**SI-LIANG LI** was born in 1994. He is currently pursuing the Ph.D. degree with the School of Mechanical Engineering, Tongji University. His research interests include precision measurement technology and robot technology.



**HAI-JIANG LIU** was born in 1976. He received the B.S., M.S., and Ph.D. degrees in mechanical engineering from Chongqing University. He is currently a Professor and a Doctoral Supervisor with the School of Mechanical Engineering, Tongji University. His research interests include intelligent manufacturing technology and precision measurement technology.



**ZE-YU XU** was born in 1995. He is currently pursuing the Ph.D. degree with the School of Mechanical Engineering, Tongji University. His research interests include robot control theory and automotive engineering technology research.



**JIN-SONG LIU** was born in 1995. He received the B.S. degree from the School of Mechanical Engineering, Jilin University and the M.S. degree from the School of Mechanical Engineering, Tongji University. His research interests include precision measurement technology and robot technology.

• • •